

# THE PRODUCTION OF HIGH QUALITY ELECTRON BEAMS IN THE ALPHA-X LASER WAKEFIELD ACCELERATOR

S. M. Wiggins<sup>#</sup>, G. H. Welsh, R. C. Issac, E. Brunetti, R. P. Shanks, S. Cipiccia, M. P. Anania, G. G. Manahan, C. Aniculaesei, B. Ersfeld, M. R. Islam, D. A. Jaroszynski, SUPA, Department of Physics, University of Strathclyde, Glasgow G4 0NG, United Kingdom  
 W. A. Gillespie, SUPA, School of Engineering, Physics and Mathematics, University of Dundee, Dundee DD1 4HN, United Kingdom  
 A. M. MacLeod, School of Computing and Creative Technologies, University of Abertay Dundee, Dundee DD1 1HG, United Kingdom

## Abstract

The ALPHA-X laser wakefield accelerator beam line comprises a high power (900 mJ, 35 fs) Ti:sapphire laser pulse, a gas jet (length 2 mm, plasma density  $\sim 10^{19} \text{ cm}^{-3}$ ) accelerating structure and a suite of single-shot electron beam diagnostics. Monoenergetic electron beams with central energy up to 220 MeV are generated in the accelerator. By operating close to the threshold for injection with low beam charge ( $\sim 1\text{-}10 \text{ pC}$ ), resolution-limited values for the measured relative energy spread (0.7%) and normalised transverse emittance ( $1.1 \pi \text{ mm mrad}$ ) demonstrate the high quality possessed by the electron bunches, making them suitable for application.

## INTRODUCTION

The laser wakefield accelerator (LWFA) mechanism, first proposed just over thirty years ago by Tajima and Dawson [1], is an attractive alternative to RF acceleration technology. High profile publications have reported the generation of quasi-monoenergetic electron beams with energy of 100s of MeV from mm-scale gas jets [2-4] and with energy of 1 GeV from cm-scale capillary discharge waveguides [5], as well as demonstrations of LWFA-driven undulator radiation sources [6,7].

Generating coherent radiation from a magnetic undulator is of particular concern for the Advanced Laser-Plasma High-Energy Accelerators towards X-rays (ALPHA-X) programme based at Strathclyde [8]. The next challenge is to advance from synchrotron-like spontaneous radiation emission [6] to free-electron laser (FEL) stimulated emission where the peak brilliance of the photon beam is enhanced by several orders of magnitude. This requires generation and transport of an electron beam of high quality (low energy spread, low transverse emittance, high peak current), matching those of conventional RF accelerators that routinely deliver such beams as drivers of the large scale X-ray self-amplified spontaneous emission FELs [9] that are now becoming operational, such as the LCLS [10]. On the ALPHA-X beam line, we have developed high quality electron beam diagnostics to allow careful characterisation of the LWFA electron beams and

demonstrate the viability of the LWFA as a driver of next generation radiation sources.

## EXPERIMENTAL SETUP

The experimental setup is shown in Fig. 1: electrons are accelerated in a relativistically self-guiding plasma channel formed in a helium gas jet (nozzle diameter 2 mm, plasma density  $\approx 1\text{-}5 \times 10^{19} \text{ cm}^{-3}$ ) by Ti:sapphire laser pulses ( $\lambda = 800 \text{ nm}$ , energy = 900 mJ, pulse duration = 35 fs). The laser beam has a  $20 \mu\text{m}$  waist (radius at  $1/e^2$ ) at the focus just inside the leading edge of the gas jet and the initial normalised vector potential  $a_0 = 1.0$ .

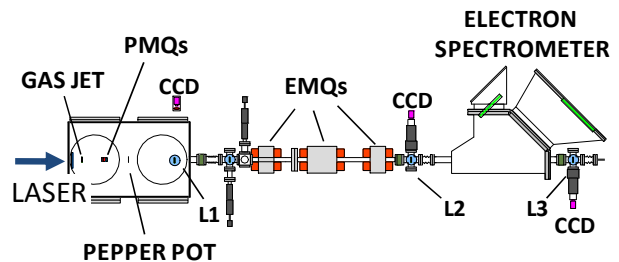


Figure 1: Setup of the ALPHA-X wakefield accelerator beam line.

Electrons are self-injected from the background plasma into the plasma density wake (bubble) trailing behind the laser pulse through the combined action of the ponderomotive force of the laser and the plasma restoring force. Permanent magnet quadrupoles (PMQs) and electromagnet quadrupoles (EMQs) are used to collimate the electron beam emerging from the plasma.

A suite of diagnostics allows the beam to be fully characterised. Pop-in Lanex screens (L1, L2 and L3 in Fig. 1) imaged by CCD cameras are used as beam profile monitors. A pop-in tungsten pepper pot mask is used to measure the r.m.s. transverse emittance of the beam. This mask consists of a  $27 \times 27$  matrix of holes with a  $25 \mu\text{m}$  mean diameter and a scintillating Ce:YAG crystal is used as the imaging screen. Measurements of electron energy spectra have been carried out using a high resolution magnetic dipole spectrometer. Ce:YAG crystals

positioned at the focal plane are used to image electrons exiting the spectrometer field. Imaging plates determine the absolute charge in the beam and can be positioned at various locations along the beam line for cross-correlation with other detector screens. Transition radiation, produced upon passing the beam through metal foils, is used to estimate the bunch length.

## RESULTS

The electron beam profile, as recorded on Lanex screen L1 located 0.6 m after the accelerator, shows that the typical beam pointing is 4-8 mrad both vertically and horizontally with standard deviation of 2-3 mrad along both axes [11]. The high energy bunch of interest has a typical divergence of 1-3 mrad. Both the pointing angle and the fluctuation are reduced when the PMQs are in-line, as shown in Fig. 2(a) and (b). This enables transportation downstream of the electron beam on almost every shot.

A crucial aspect of the ALPHA-X programme is development of a LWFA-driven FEL and this requires optimal beam transport from source to undulator. Fig. 2(c) shows an electron beam profile at Lanex screen L3, located 0.2 m before our undulator (not shown in Fig. 1). The beam size is consistent with beam transport simulations indicating electron beam focusing near the centre of the undulator and matched to its length [12].

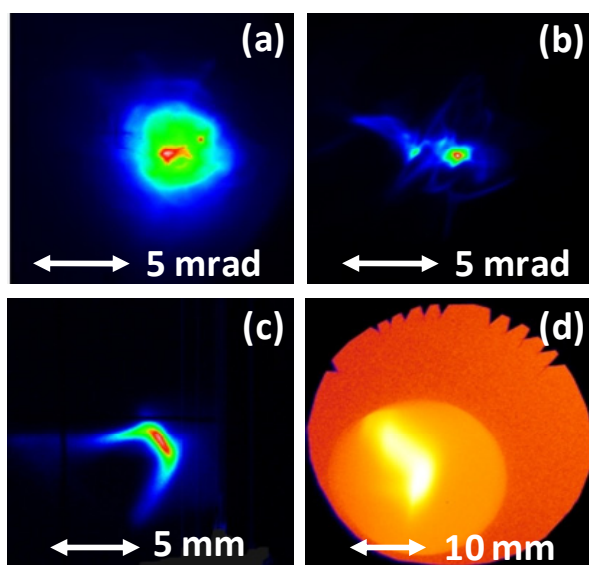


Figure 2: False-colour electron beam images captured on (a) Lanex screen L1 without PMQ collimation, (b) Lanex screen L1 with PMQ collimation, (c) Lanex screen L3 and (d) an imaging plate showing charge of 3.1 pC.

Absolute charge measurements have been conducted using imaging plates (Fujifilm, BAS-SR2025) inserted into the beam line, as shown in Fig. 2(d). Cross-calibration has been achieved for each Lanex screen simply with simultaneous capture on each one in turn while the stability of the accelerator enables statistical

averaging over a large number of shots to be performed for calibration of the YAG screen in the electron spectrometer. The total beam charge can reach 30 pC but the monoenergetic peak bunch of interest typically contains 1-10 pC. An r.m.s. bunch duration of 2 fs is indicated by transition radiation measurements, hence, it is seen that the peak current can reach a few kA.

The best quality electron beams are obtained for lower charge, i.e., when the self-injection process in the accelerator is close to threshold. This ensures that the phase-space volume for injection is small such that the resultant emittances are low. Control of the plasma density (position of laser with respect to gas nozzle and gas backing pressure) and/or laser parameters (energy, focal spot size, pulse duration) enables narrow energy spread electron spectra to be obtained over a wide of energies for the 2 mm long gas jet accelerator. The central energy of the main electron bunch is typically in the range 130-170 MeV, as shown in Fig. 3(a) and (b) and stability over a run of consecutive shots is as low as 3% [11].

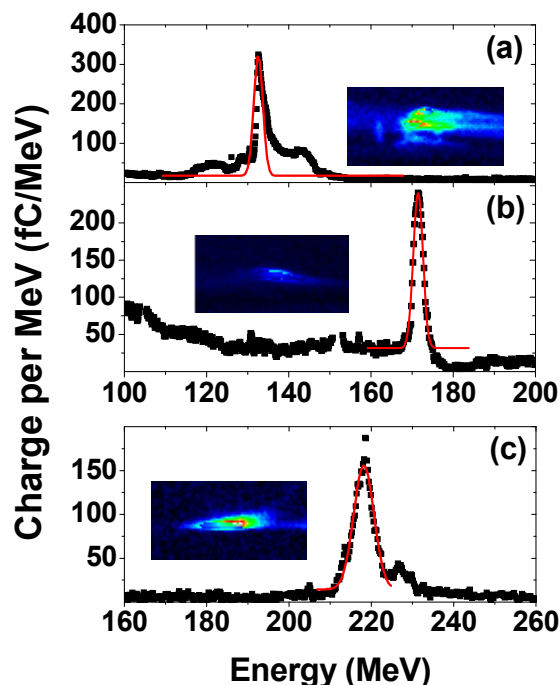


Figure 3: Electron energy spectra showing a bunch (respective false-colour YAG image inset) with (a) central energy = 133 MeV and measured  $\sigma_v/\gamma = 0.8\%$ , (b) central energy = 171 MeV and measured  $\sigma_v/\gamma = 0.7\%$  and (c) central energy = 218 MeV and measured  $\sigma_v/\gamma = 1.1\%$ . Each red curve is a Gaussian fit and the charge in each bunch is  $\sim 0.5$  pC.

At higher plasma density  $\approx 4-6 \times 10^{19} \text{ cm}^{-3}$ , the central electron energy decreases to around 70 MeV [11] while, at lower density  $\approx 0.8-1 \times 10^{19} \text{ cm}^{-3}$ , the central electron energy has reached as high as 218 MeV [Fig. 3(c)]. The latter observation means that our accelerator has passed the 1 GeV/cm figure-of-merit for the accelerating

gradient. At these plasma densities, the laser  $a_0$  parameter is indicated to increase to  $\sim 2.4$ , which is close to that expected because of self-focusing and photon acceleration effects [13].

The measured r.m.s. relative energy spread  $\sigma_\gamma/\gamma$  is as low as 0.4-1.0% which is very close to the resolution limit of the spectrometer. Simultaneous measurement of the energy spectrum and emittance/divergence is not possible but beam transport simulations show that the actual relative energy spread is estimated to be as low as  $\sim 0.3\%$  [11]. For such narrow energy spreads, the transverse emittance strongly influences the imaging quality and resolution of the spectrometer.

The normalised transverse emittance  $\varepsilon_N$  inferred from the spectral diagnostic (less than  $\sim 0.5 \pi$  mm mrad) is consistent with the pepper pot mask measurements conducted on the beam line. An example image of the mask-generated data is shown in Fig. 4. The relatively thin mask (thickness of  $125 \mu\text{m}$  that is less than the stopping distance for  $\sim 100$  MeV electrons) acts as a scattering element for electrons passing through the bulk material. This creates a uniform background distribution that can be readily subtracted to provide clean beamlet signals.

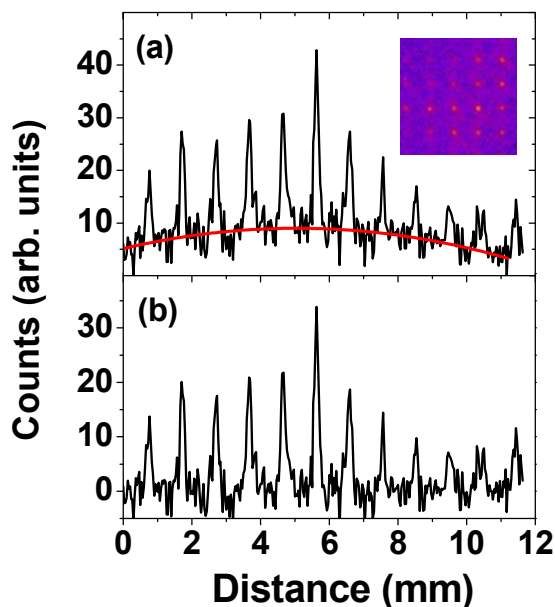


Figure 4: Pepper pot transverse line-outs for (a) the raw data from the YAG image, part of which is inset, with the red curve depicting the best-fit background and (b) the background-corrected data. These data correspond to a normalised transverse emittance of  $1.3 \pi$  mm mrad for an electron beam energy of 125 MeV.

The measured  $\varepsilon_N$  is found to be as low as  $1.1 \pi$  mm mrad with ellipticity in the beam profile also evident [14]. This single-shot diagnostic is being upgraded for future experiments with refinement of the mask geometry, the imaging screen spatial resolution and the drift distance

between mask and imaging screen. Applicability up to an electron energy of  $\sim 300$  MeV is achievable with an increased mask thickness of  $250 \mu\text{m}$ .

## CONCLUSIONS

In conclusion, we have demonstrated the production of high quality electron beams on the ALPHA-X laser wakefield accelerator. The key beam parameters, energy spread and transverse emittance, are found to be less than 1% and  $\sim 1.0 \pi$  mm mrad respectively, both limited by detection system resolution. With charge in the range 1-10 pC and a bunch length of a few femtoseconds, the peak current is estimated to be  $\sim$  kA.

Based on our experimental parameters, FEL gain should be observable in the vacuum ultra-violet wavelength range with extension into the XUV range on the horizon. Wide tunability of the electron energy from the gas jet accelerator can also be achieved, illustrating the potential of the LWFA as a flexible source for user communities.

## ACKNOWLEDGEMENTS

We acknowledge the support of the U. K. EPSRC, the EC's Seventh Framework Programme (LASERLAB-EUROPE/LAPTECH, grant agreement no. 228334) and the Extreme Light Infrastructure (ELI) project.

## REFERENCES

- [1] T. Tajima and J. M. Dawson, Phys. Rev. Lett. 43 (1979) 267.
- [2] S.P.D. Mangles et al., Nature (London) 431 (2004) 535.
- [3] C.G.R. Geddes et al., Nature (London) 431 (2004) 538.
- [4] J. Faure et al., Nature (London) 431 (2004) 541.
- [5] W.P. Leemans et al., Nature Phys. 2 (2006) 696.
- [6] H.-P. Schlenvoigt et al., Nature Phys. 4 (2008) 130.
- [7] M. Fuchs et al., Nature Phys. 5 (2009) 826.
- [8] D.A. Jaroszynski et al., Phil. Trans. R. Soc. A 364 (2006) 689.
- [9] J. Feldhaus, J. Arthur and J. B. Hastings, J. Phys. B: At. Mol. Opt. Phys. 38 (2005) S799.
- [10] L. Young et al., Nature (London) 466 (2010) 56.
- [11] S. M. Wiggins et al., Plasma Phys. Control. Fusion 52 (2010) 124032.
- [12] M.P. Anania et al., Proc. SPIE 7359 (2009) 735916.
- [13] A.J.W. Reitsma, R. A. Cairns, R. Bingham, and D. A. Jaroszynski, Phys. Rev. Lett. 94, (2005) 085004.
- [14] E. Brunetti et al., Phys. Rev. Lett. 105 (2010) 215007.